Collective Plasmon–Molecule Excitations in Nanojunctions: Quantum Consideration

3 AUTHORS:

Alexander James White
Los Alamos National Laboratory
11 PUBLICATIONS   **86** CITATIONS

SEE PROFILE

Boris D. Fainberg
Holon Institute of Technology
104 PUBLICATIONS   **529** CITATIONS

SEE PROFILE

Michael Galperin
University of California, San Diego
82 PUBLICATIONS   **2,540** CITATIONS

SEE PROFILE

Collective Plasmon-Molecule Excitations in Nanojunctions: Quantum Consideration

Alexander J. White,[†] Boris D. Fainberg,[‡] and Michael Galperin*[,†]

[†]Department of Chemistry & Biochemsitry, University of California at San Diego, La Jolla, California 92093, United States
[‡]Faculty of Sciences, Holon Institute of Technology, Holon 58102, Israel

S *Supporting Information*

ABSTRACT: We present a pseudoparticle nonequilibrium Green function formalism as a tool to study the coupling between plasmons and excitons in nonequilibrium molecular junctions. The formalism treats plasmon-exciton couplings and intramolecular interactions exactly and is shown to be especially convenient for exploration of plasmonic absorption spectrum of plexitonic systems, where combined electron and energy transfers play an important role. We demonstrate the sensitivity of the molecule-plasmon Fano resonance to junction bias and intramolecular interactions (Coulomb repulsion and intramolecular exciton coupling) and compare our predictions for nonlinear optical effects to previous studies. Our study opens a way to deal with strongly interacting plasmon-exciton systems in nonequilibrium molecular devices.

SECTION: Physical Processes in Nanomaterials and Nanostructures
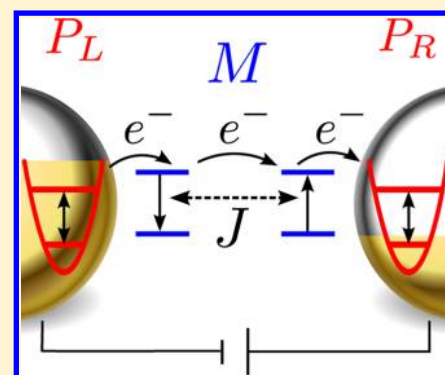
Recent progress in nanofabrication techniques and advances in laser technologies opened new directions in research of plasmonic materials on the nanoscale.[1,2] Nanoplasmonics finds its application in optical devices,[3–6] photovoltaics,[7–9] and biology.[10–13] In particular, field enhancement by surface plasmons on the nanoscale allows the detection of optical response in current carrying molecular junctions.[14] Plasmon coupling to molecular excitations[15] is studied by a field of research named plexcitonics.[16] Such couplings yield a possibility for coherent control of molecular systems[17,18] and are utilized in molecular photodevices.[19–21]

Advances in experimental techniques has caused a surge of theoretical research in the areas of nanoplasmonics and plexcitonics. Usually plasmon excitations are studied utilizing the laws of classical electrodynamics,[22–26] whereas the molecular system is treated quantum-mechanically.[27–32] We used a similar scheme to study transport in molecular junctions driven by surface plasmons.[33,34] Recently, quantum descriptions of plasmonic excitatitons started to appear. For example, time-dependent density functional theory was employed to simulate plasmon excitations in relatively small metallic clusters in refs 35−38, whereas ref 39 utilized a quantum master equation to study the effect of plasmonic excitations on the current.

The observation of Fano resonances[40] in plasmonic nanostructures[41] gave impetus to a quantum description of excitations. Such considerations have been done for quantum-dot−metal nanoparticle system, where the metal nanoparticle was studied classically while oscillations of the quantum dot were treated within a density matrix approach.[42–44] Recently, a fully quantum description of the model was reported in ref 45.

Finally, a mean-field quantum study of the dips in the absorption spectrum of a molecule between a pair of metallic spheres was presented in ref 46 within an equilibrium Green function formalism. It relies on the factorization of the collective excitations into separated plasmonic and molecular contributions. In this respect, it is good to bear in mind that the dips discussed in ref 46 can arise from both Fano-like interference and hybridization of a molecule dipole and the plasmon resonances.[47] Strong hybridization is related to the physics of avoided crossing of diabatic states corresponding to the molecular resonance and plasmon and gives rise to a new quasiparticle − the polariton.[48–50] Thus, the mean-field type factorization of the molecular and plasmon excitations is not safe in the case of strong plasmon-exciton coupling.

Here we consider collective plasmon-molecule excitations in a junction, where a molecule (M) is placed between two nanoparticles (L and R), each representing a contact. The molecule, modeled as a chain of D two-level systems, exchanges electrons and energy with the contacts. Energy exchange is modeled as exciton-plasmon coupling within the dipole approximation. Both the molecule and plasmons are treated quantum mechanically. We employ a pseudoparticle non-equilibirum Green function (NEGF) formalism, described in detail in our recent publication.[51] The formalism allows us to generalize the consideration of ref 46 to a nonequilibrium, finite temperature situation, and to treat the system part (molecule

and plasmons) exactly. The latter is important in the case of strong plasmonic coupling to molecular excitations. We evaluate the absorption spectrum of the junction and discuss the influence of bias and intramolecular interactions (Coulomb repulsion, U, and exciton hopping, J) on the spectrum.

The Hamiltonian of the junction is (here and below $\hbar = 1$)

$$\hat{H} = \hat{H}_M + \hat{H}_P + \hat{V}_{MP} + \sum_{K=L,R,rad} (\hat{H}_K + \hat{V}_K) \tag{1}$$

Here $\hat{H}_M$ is the molecular Hamiltonian

$$\hat{H}_M = \sum_{c=1}^{D} \left[\sum_{s=g,e} \varepsilon_s \hat{c}_{cs}^\dagger \hat{c}_{cs} + \frac{U}{2} \hat{N}_c (\hat{N}_c - 1) \right] + \sum_{c=1}^{D-1} \left[-\sum_{s=g,e} t_s \hat{c}_{cs}^\dagger \hat{c}_{(c+1)s} + J\hat{b}_c^\dagger \hat{b}_{c+1} + H.c. \right] \tag{2}$$

$\hat{H}_P$ models plasmonic excitations in the nanoparticles as two coupled dipoles, L and R,

$$\hat{H}_P = \sum_{K=L,R} \Omega_K \hat{b}_K^\dagger \hat{b}_K - (\Delta_{PP} \hat{b}_R^\dagger \hat{b}_L + H.c.) \tag{3}$$

and $\hat{V}_{MP}$ describes the exciton-plasmon coupling

$$\hat{V}_{MP} = -\sum_{c=1}^{D} \sum_{K=L,R} (\Delta_{cK} \hat{b}_c^\dagger \hat{b}_K + H.c.) \tag{4}$$

The contacts L and R are modeled as reservoirs of free electrons

$$\hat{H}_K = \sum_{\kappa \in K} \varepsilon_\kappa \hat{c}_\kappa^\dagger \hat{c}_\kappa \quad (K = L, R) \tag{5}$$

and $\hat{H}_{rad}$ introduces the radiation field

$$\hat{H}_{rad} = \sum_\alpha \omega_\alpha \hat{a}_\alpha^\dagger \hat{a}_\alpha \tag{6}$$

$\hat{V}_K$ ($K = $L,R) and $\hat{V}_{rad}$ describe the electron transfer between the molecule and contacts and the plasmons and molecular excitations coupling to the radiation field, respectively

$$\hat{V}_K = \sum_{\substack{\kappa \in K \\ s=g,e}} (V_{\kappa s} \hat{c}_\kappa^\dagger \hat{c}_{c_K s} + H.c.) \tag{7}$$

$$\hat{V}_{rad} = \sum_{\alpha; K \in \{L,1,...,D,R\}} (W_{\alpha K} \hat{a}_\alpha^\dagger \hat{b}_K + H.c.) \tag{8}$$

where $c_K = 1$ (D) for $K = $L (R). Note that for simplicity we ignore the quadrupole mode of the plasmons described in ref 46. This simplification does not influence the physics of the Fano resonance discussed below (see Supporting Information).

In eqs 2–8 $\hat{c}_{cs}^\dagger$ ($\hat{c}_{cs}$) and $\hat{c}_\kappa^\dagger$ ($\hat{c}_\kappa$) are creation (annihilation) operators for an electron in the molecular orbital s at the site c of the chain and contact state κ, respectively, and $\hat{a}_\alpha^\dagger$ ($\hat{a}_\alpha$) is the creation (annihilation) operator for a photon in mode α of the radiation field. $\hat{b}_K^\dagger$($\hat{b}_K$) creates (destroys) plasmons in a nanoparticle ($K = $L,R) or excitons at a site $c = 1,...,D$ of the molecule ($K = c$, $\hat{b}_c^\dagger \equiv \hat{c}_{ce}^\dagger \hat{c}_{cg}$). $\hat{N}_c \equiv \sum_{s=g,e} \hat{c}_{cs}^\dagger \hat{c}_{cs}$ is the total charge of the site c.

Below we consider molecular chains of one ($D = 1$) and two ($D = 2$) sites. The first model is used to extend the consideration of ref 46 to nonequilibrium and beyond the mean-field type of treatment. The second allows us to consider

influence of intramolecular energy exchange on the absorption spectrum of the junction. In particular, we examine features of exciton compensation of the Coulomb blockade[52] in the plasmon spectrum. Note that, in principle, the model (eqs 1–8) is capable of describing the optical spectrum features related to Kondo physics. However, such consideration requires going beyond the lowest order in the system-bath coupling (the noncrossing approximation) employed below and is not presented here.

Following ref 46 we seek to calculate the correlation function

$$P(\tau, \tau') = -i \langle T_c \hat{D}(\tau) \hat{D}^\dagger(\tau') \rangle \tag{9}$$

of the bonding dipolar mode, $\hat{D} = \hat{b}_L + \hat{b}_R$, which implies that the two nanoparticles absorb photons in the same phase. This is appropriate when assuming the incident photon field is perpendicular to the nanoparticle dimer axis.[46] Because we consider a nonequilibrium situation, the Green function in eq 9 is defined on the Keldysh contour. τ and τ' are contour variables, and T_c is the contour ordering operator.

We assume that only one mode of the radiation field, ω_0, pumps the system. All other modes of the radiation bath are empty. Moreover, the pumping mode is coupled to the bonding dipolar mode, eq 9, and direct coupling to the molecule is neglected. Absorption at the laser frequency, ω_0, is given by a photon influx into the system, which at steady state is (see Supporting Information)[53]

$$I_{abs}(\omega_0) = -\int_0^\infty \frac{d\omega}{2\pi} \gamma(\omega) N_{\omega_0}(\omega) \, \text{Im} \, P^>(\omega) \tag{10}$$

where $\gamma(\omega) = \sum_{K=L,R} \gamma_K(\omega) \equiv 2\pi \sum_{K=L,R} \sum_\alpha |W_{K\alpha}|^2 \delta(\omega - \omega_\alpha)$ is the total plasmon dissipation rate,

$$N_{\omega_0}(\omega) \equiv N_0 \frac{1}{\pi} \frac{\delta^2}{(\omega - \omega_0)^2 + \delta^2} \tag{11}$$

is the laser-induced mode population (δ is the laser bandwidth), and $P^>(\omega)$ is the Fourier transform of the greater projection of $P(\tau, \tau')$, eq 9.

Here we briefly outline the pseudoparticle approach for energy and electron transfer in junctions. For an in-depth description, see, for example, ref 51 and references therein. The total Hamiltonian, ref 1, is separated into the system, eqs 2–4, and bath, eqs 5 and 6, parts. The system Hamiltonian is represented on a basis of many-body states $\{|m\rangle\}$ (this may be the eigenbasis of the system, or any other complete set of many-body states in the system subspace), and thus all interactions in the system subspace are treated exactly. Every creation $\hat{O}_\nu^\dagger$ (annihilation $\hat{O}_\nu$) operator in the system is expressed in terms of *pseudoparticles* via spectral decomposition

$$\hat{O}_\nu^\dagger \equiv \sum_{m_1, m_2} O_{m_1 m_2}^\nu \hat{d}_{m_1}^\dagger \hat{d}_{m_2} \tag{12}$$

where $O_{m_1 m_2}^\nu \equiv \langle m_1 | \hat{O}_\nu^\dagger | m_2 \rangle$. The pseudoparticle operator $\hat{d}_m^\dagger$ creates the many-body state $|m\rangle = \hat{d}_m^\dagger |0\rangle$ ($|0\rangle$ is vacuum state). These operators follow the usual boson/fermion commutation relations within an extended Hilbert space. To specify the physical subspace, the constraint

$$\hat{Q} = \sum_m \hat{d}_m^\dagger \hat{d}_m = 1 \tag{13}$$

must be applied. In the extended Hilbert space the pseudoparticle Green's function

$$G_{mm'}(\tau, \tau') = -i\langle T_c \hat{d}_m(\tau) \hat{d}_{m'}^{\dagger}(\tau') \rangle \qquad (14)$$

satisfies the usual Dyson equation, $\mathbf{G} = \mathbf{g} + \mathbf{g}\boldsymbol{\Sigma}\mathbf{G}$, where $\boldsymbol{\Sigma}$ is the pseudoparticle self-energy due to the coupling to the baths, eqs 7 and 8. (See the Supporting Information for details.)

The Green function in eq 9 is obtained utilizing eq 12. We need its greater projection to calculate the absorption spectrum in eq 10. The explicit expression is

$$P^>(\omega) = \sum_{\substack{K,K' \in \{L,R\} \\ m_1,m'_1,m_2,m'_2 \in M}} \tilde{\chi}_{m_1m_2}^{*K} \chi_{m'_1m'_2}^{K'} \zeta_{m_2} \times \int_{-\infty}^{\infty} dE$$
$$\frac{-1}{\pi} \text{Im}[G_{m_1m'_1}^r(E+\omega)] G_{m'_2m_2}^<(E) \qquad (15)$$

where $\chi_{m_1m_2}^{K} \equiv \langle m_1|\hat{b}_K^{\dagger}|m_2\rangle$ and $\zeta_m = 1\ (-1)$ if state $|m\rangle$ is bosonic (fermionic), and $G^{r(<)}$ are the retarded (lesser) projections of the pseudoparticle Green function, eq 14.

Here we present the results of numerical simulations for the model, eq 1, which demonstrate the effect of electron transport on the plasmon absorption spectrum, and, in particular, on the Fano resonance.[40] Following ref 46, most of the calculations below are performed in the optical linear response regime (optical linear response corresponds to disregarding effect of laser on the system), with nonlinear optical effects shown in Figure 2.

To make our calculations representative of a realistic junction, we use the parameters proposed in ref 46. Unless otherwise specified, the parameters are $T = 300$ K, $\varepsilon_e = -\varepsilon_g = 1.6$ eV, $U = 1$ eV, $\Omega_L = \Omega_R = 3.49$ eV, and $\Delta_{PP} = 125$ meV. Below, for $D = 1$, we follow ref 46, taking $\Delta_{1L} = \Delta_{1R} = 20$ meV. For molecular dimer ($D = 2$) this parameter represents coupling to the closest plasmon, $\Delta_{1L} = \Delta_{2R} = 20$ meV. To estimate the coupling to the other plasmon, we take into consideration that the electric field created by the dipole plasmon varies as $\sim 1/r^3$ (r is the distance from the center of the sphere).[54] Then, for the parameters of ref 46 and taking the distance between the molecules in the dimer ~ 1 nm, we get $\Delta_{1R} = \Delta_{2L} = 15.75$ meV. The electron escape rate to the contacts is $\Gamma_{c_KS}^{K} = 1$ meV ($K = $ L,R, $s = $ g,e), the dissipation rates are $\gamma_L = \gamma_R = 86$ meV for the plasmons and $\gamma_M = 4$ meV for the molecular exciton(s). The laser bandwidth is $\delta = 1$ meV. The Fermi energy is chosen at the origin, $E_F = 0$, and bias V_{sd} shifts the chemical potentials in the contacts as $\mu_L = E_F + \eta V_{sd}$ and $\mu_R = E_F - (1-\eta)V_{sd}$. Here η is the voltage division factor. Below we consider symmetric, $\eta = 0.5$, and asymmetric, $\eta = 1$, bias divisions.

Single Molecule (D = 1). We work in the basis of many-body states $|S_M,P_L,P_R\rangle$ characterized by the states of the molecule $S_M \in \{0,g,e,2\}$ and excitation states of the plasmons $P_{L,R} \in \{0,1,2,...\}$. At equilibrium, the principle optical transition that controls the absorption spectrum is between the ground state, $|g,0,0\rangle$ and two excited plasmon states, $|g,1,0\rangle$ and $|g,0,1\rangle$. The coupling, Δ_{MP}, between $|g,1,0\rangle$ ($|g,0,1\rangle$) and $|e,0,0\rangle$ is the origin of the Fano resonance in the absorption spectrum.

Figure 1 shows the effect of bias on the Fano resonance. For asymmetrically applied bias, $\eta = 1$, and in the absence of Coulomb repulsion, $U = 0$, both neutral, $|g,0,0\rangle$, and anion, $|2,0,0\rangle$, molecular states become equally populated above the threshold, $\mu_L = \varepsilon_e$. Because the anion state cannot exchange energy with the plasmons, the Fano resonance decreases to ~50% relative to its equilibrium value. (See Figure 1b.)
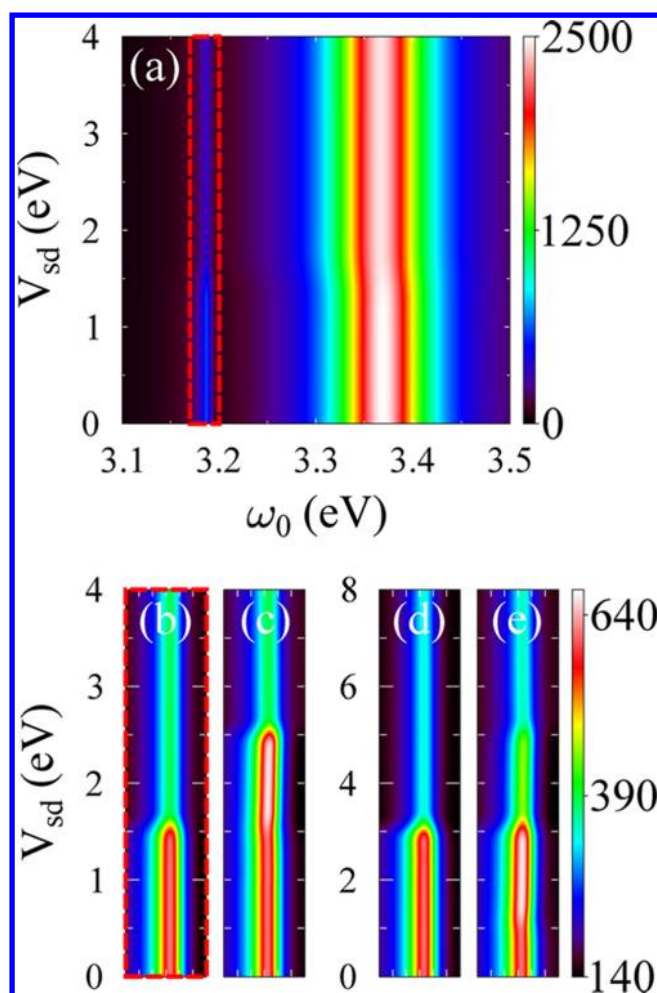

Figure 1. Plasmon absorption spectrum $I_{abs}(\omega_0)/\gamma N_0 \delta$, eq 10, as a function of bias V_{sd} (a) and close-up of the Fano resonance (b–e). Calculations with asymmetrically applied bias, $\eta = 1$, are performed with $U = 0$ in panels a and b and $U = 1$ eV in panel c. Results for symmetrically applied bias, $\eta = 0.5$, are shown in (d) $U = 0$ and (e) $U = 1$ eV. See text for other parameters.

Finite Coulomb repulsion causes this transition to shift by U to higher biases. (See Figure 1c.) Moreover, in the region $\varepsilon_e < \mu_L < \varepsilon_e + U$, the Fano resonance increases. This is due to a partial blocking of the virtual transition from $|g,1,0\rangle$ ($|g,0,1\rangle$) via $|e,0,0\rangle$ to $|0,0,0\rangle$ by the Fermi distribution in the left contact. The blocking renormalizes the local density of the $|g,1,0\rangle$ and $|g,0,1\rangle$ states, which are responsible for the Fano resonance. Note that this is a combined electron/energy transfer mechanism, which is readily accounted for by the pseudoparticle NEGF formalism. Note also that in the standard NEGF formalism a fourth-order perturbation theory is required to take the effect into account.

We next consider a symmetrically coupled junction, $\eta = 0.5$. In the absence of Coulomb repulsion, $U = 0$, reaching the threshold results in equal population for all molecular states: cation $|0,0,0\rangle$, neutral ground $|g,0,0\rangle$, neutral excited $|e,0,0\rangle$, and anion $|2,0,0\rangle$. This would imply reduction in Fano resonance to ~25% of its equilibrium height. The observed reduction of ~40% (Figure 1d) is due to the energy transfer between molecule and plasmon (and strong dissipation of the plasmon), which causes quick relaxation of the molecular exciton $|e,0,0\rangle$,

thus increasing the population of to the neutral ground state $|g,0,0\rangle$.

Finite U reveals four distinct Fano resonance regions (Figure 1e): (1) Below threshold $V_{sd} < \varepsilon_e - \varepsilon_g - 2U$, Fano resonance has its equilibrium appearance. (2) For $\varepsilon_e - \varepsilon_g - 2U < V_{sd} < \varepsilon_e - \varepsilon_g$, the virtual transition from $|g,1,0\rangle (|g,0,1\rangle)$ via $|e,0,0\rangle$ to $|2,0,0\rangle$ is blocked from the right contact, because $\mu_R - \varepsilon_g < U$. This results in an increase in the Fano resonance due to a local density of states renormalization by an electron/energy transfer mechanism (similar to that discussed in Figure 1c). (3) For $\varepsilon_e - \varepsilon_g < V_{sd} < \varepsilon_e - \varepsilon_g + U$, three molecular states (cation $|0,0,0\rangle$, neutral ground $|g,0,0\rangle$, and neutral excited $|e,0,0\rangle$) become accessible. Quick relaxation of the molecular exciton, $|e,0,0\rangle \rightarrow |g,0,0\rangle$, results in a population of the neutral ground state ~2/3, leading to a corresponding decrease in the Fano resonance relative to its equilibrium value (see discussion of Figure 1d). (4) For $V_{sd} > \varepsilon_e - \varepsilon_g + U$, all four molecular states are accessible, and the Fano resonance reduces to ~40% of its equilibrium value.

Thus Figure 1 demonstrates sensitivity of the Fano resonance to nonequilibrium conditions, which renormalize the local molecular density of states resulting in measurable consequences for the absorption spectrum of the system. Note that the effect requires taking into account coherently coupled electron and energy-transfer processes in an open non-equilibrium molecular system. The pseudoparticle NEGF is a convenient tool for such studies.

Figure 2 presents simulation beyond the optical linear response regime. Calculations are done at $V_{sd} = 0$; other
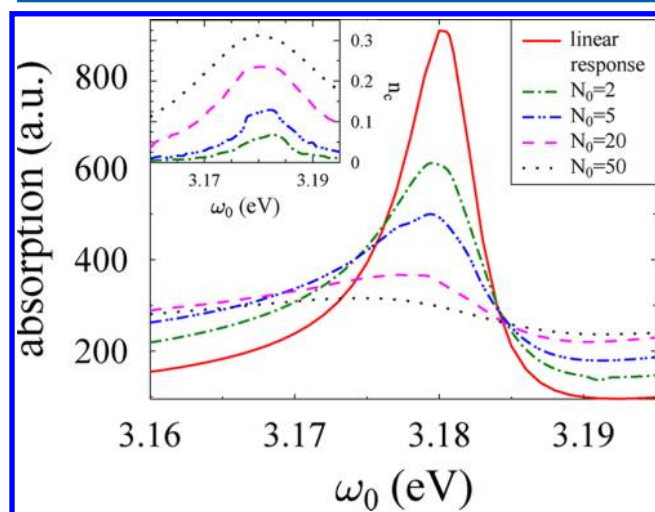

Figure 2. Nonlinear effects in the plasmon absorption: $I_{abs}(\omega_0)/\gamma N_0 \delta$, eq 10, for different intensities of laser field. Inset shows the population, n_c, of the molecular excited state $|e,P_L,P_R\rangle$. See text for parameters.

parameters are as in Figure 1. Here the laser field is fully taken into account. Increase in the intensity of the laser results in population of the excited state of the molecule (see inset) and suppression of Fano resonance. Note, however, that contrary to predictions of ref 46 the Fano resonance is suppressed already for $n_c = 0.3$. The reason is additional broadening of the resonance due to coupling to the pumping mode, disregarded in previous treatment. Moreover, because population of the excited state is different at different frequencies of the laser, the slope of the Fano resonance also depends on the intensity of the laser field. So, utilizing linear response theory in studies of

optical spectrum of molecular junctions, where hot spots yield strongly enhanced local fields, is not always justified.

Molecular Dimer (D = 2). A molecular dimer allows for the comparison of two energy-transfer mechanisms: the intra-molecular and molecule-plasmon. Here the many-body states are $|S_1,S_2,P_L,P_R\rangle$, where S_1 and S_2 describe states of the first and second molecule. We use the following parameters: $t_e = t_g = 5$ meV and $U = 2$ eV. Other parameters are as in Figure 1.

Figure 3 demonstrates the effect of intramolecular exciton coupling, J, on the absorption spectrum at large symmetric bias,
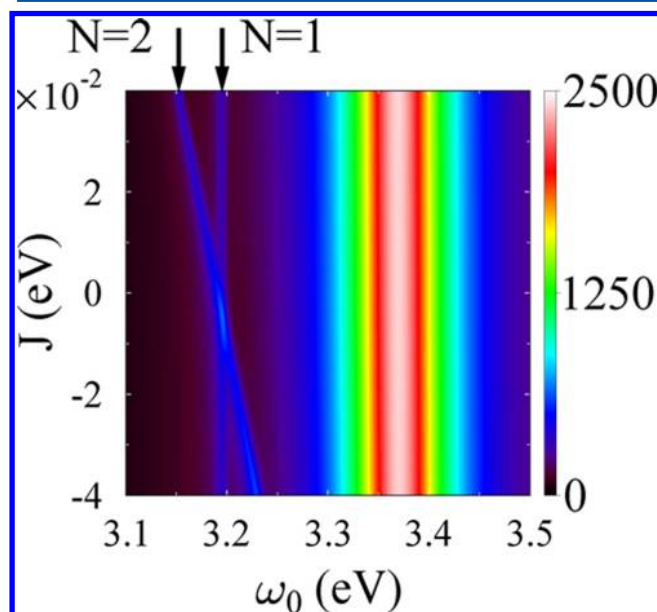

Figure 3. Plasmon absorption spectrum $I_{abs}(\omega_0)/\gamma N_0 \delta$, eq 10, as a function of J at symmetrically applied bias of $V_{sd} = 6$ eV. Arrows indicate the Fano resonances attributed to the $N = 1$ and 2 charge blocks of the system. See text for parameters.

$\eta = 0.5$ and $V_{sd} = 6$ eV. In general, the energy-transfer coupling J is controlled by electromagnetic environment that makes it complex-valued.[52] Here we consider J an independent parameter for the sake of simplicity. With these parameters, U is large enough to prevent double occupancy of either molecule, and the spectrum demonstrates two Fano resonances. The first does not change with J and is a result of the plasmon coupling to transition between the singly occupied ($N = 1$) molecular states with an electron on either site of the dimer: $|g,0,1,0\rangle (|g,0,0,1\rangle) \rightarrow |e,0,0,0\rangle$ or $|0,g,1,0\rangle (|0,g,0,1\rangle) \rightarrow |0,e,0,0\rangle$. The second peak is attributed to the plasmon coupling to transition between doubly occupied ($N = 2$) states with both sites populated by one electron: $|g,g,1,0\rangle (|g,g,0,1\rangle) \rightarrow |e,g,0,0\rangle$ $(|g,e,0,0\rangle)$. These excited molecular states ($|e,g,0,0\rangle$ and $|g,e,0,0\rangle$) are coupled by J, which results in a linear dependence of the Fano resonance on the intramolecular excitonic coupling. Note that such absorption signatures may provide direct measurement of J in molecular dimers.

Recently, Li et al.[52] demonstrated exciton compensation of the Coulomb blockade for a dimer system. Figure 4 shows how this physical phenomena affects the plasmon absorption spectrum. Parameters of the calculation are $t_e = t_g = 1$ meV, $U = 0.2$ eV, and $\Gamma_{c_K c}^K = 2$ meV ($K = L,R; s = g,e$). Other parameters are as in Figure 3. The Coulomb blockade is lifted when $-J \approx U$, as was discussed in ref 52 (see inset). One sees that similar behavior is observed for the Fano resonance. The
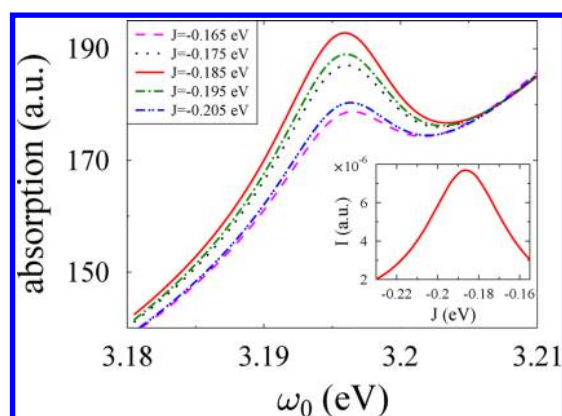
Figure 4. Fano resonance of the plasmon absorption spectrum $I_{abs}/\gamma N_0 \delta$, eq 10, for different values of J. Inset shows current I versus J. See text for parameters.

cause of enhancement of absorption spectrum is the same as that for the transport and is related to unblocking (reducing population) of the $|2,0,P_L,P_R\rangle$ state ($E \approx \varepsilon_g + \varepsilon_e + U$) when it comes into resonance with an eigenstate of the $|g,e,P_L,P_R\rangle$ and $|e,g,P_L,P_R\rangle$ pair ($E \approx \varepsilon_g + \varepsilon_e \pm J$). Therefore, the absorption spectrum measurements can be used as a source of information on the transport regime of the junction.

In conclusion, we have presented a pseudoparticle NEGF approach to study the optical properties of plasmonic systems interacting with a molecule in a current-carrying junction. The formalism is exact in its description of the model plasmon-exciton and intramolecular interactions so that collective plasmonic-molecular excitations in the strong coupling regime are treated properly. The method is an invaluable tool in describing combined electron and energy-transfer processes in the system. The latter are shown to play an important role in understanding the plasmon absorption spectrum at non-equilibrium. We demonstrated the ability to alter the Fano resonance intensity by changing the junction bias. We further discussed nonlinear effects in the spectrum and compared our results with the mean-field equilibrium study of ref 46. For a molecular dimer, we showed the sensitivity of the Fano resonances to the intramolecular exciton coupling, and discussed the possibility of revealing information on intramolecular interactions from plasmonic absorption spectrum. Finally, we showed that the effect of exciton compensation of Coulomb blockade, introduced recently in ref 52 for transport through the junction, can also be measured in the absorption spectrum. Practical implementation of the developed approach based on its combination with consistent electrodynamical calculations of the corresponding parameters will be published elsewhere.

ASSOCIATED CONTENT

Ⓢ Supporting Information

A discussion of the pseudoparticle NEGF approach and its application to the problem of plasmon-molecule excitations in nanojunctions is discussed. An extra figure related to definition of the model and derivation of eqs 10 and 15 are provided. This material is available free of charge via the Internet at http://pubs.acs.org.

AUTHOR INFORMATION

Notes

The authors declare no competing financial interest.

REFERENCES

(1) Halas, N. J. An Emerging Field Fostered by Nano Letters. *Nano Lett.* **2010**, *10*, 3816−3822.

(2) Stockman, M. I. Nanoplasmonics: Past, Present, And Glimpse into Future. *Opt. Express* **2011**, *19*, 22029−22106.

(3) Gramotnev, D. K.; Bozhevolnyi, S. I. Plasmonics beyond the Diffraction Limit. *Nat. Photon.* **2010**, *4*, 83−91.

(4) Schuller, J. A.; Barnard, E. S.; Cai, W.; Jun, Y. C.; White, J. S.; Brongersma, M. L. Plasmonics for Extreme Light Concentration and Manipulation. *Nat. Mater.* **2010**, *9*, 193−204.

(5) Hill, M. T. Status and Prospects for Metallic and Plasmonic Nano-Lasers. *J. Opt. Soc. Am. B* **2010**, *27*, B36−B44.

(6) Juan, M. L.; Righini, M.; Quidant, R.; Quidant, R. Plasmon Nano-Optical Tweezers. *Nat. Photon.* **2011**, *5*, 349−356.

(7) Atwater, H. A.; Polman, A. Plasmonics for Improved Photovoltaic Devices. *Nat. Mater.* **2010**, *9*, 205−213.

(8) Pillai, S.; Green, M. Plasmonics for Photovoltaic Applications. *Sol. Energy Mater. Sol. Cells* **2010**, *94*, 1481−1486.

(9) Catchpolea, K. R.; Mokkapatia, S.; Becka, F.; Wanga, E.-C.; McKinleya, A.; Bascha, A.; Lee, J. Plasmonics and Nanophotonics for Photovoltaics. *MRS Bull.* **2011**, *36*, 461−467.

(10) Aslan, K.; Lakowicz, J. R.; Geddes, C. D. Plasmon Light Scattering in Biology and Medicine: New Sensing Approaches, Visions and Perspectives. *Curr. Opin. Chem. Biol.* **2005**, *9*, 538−544.

(11) Sannomiya, T.; Voeroes, J. Single Plasmonic Nanoparticles for Biosensing. *Trends Biotechnol.* **2011**, *29*, 343−351.

(12) Hinterdorfer, P.; Garcia-Parajo, M. F.; Dufrene, Y. F. Single-Molecule Imaging of Cell Surfaces Using Near-Field Nanoscopy. *Acc. Chem. Res.* **2012**, *45*, 327−336.

(13) Zheng, Y. B.; Kiraly, B.; Weiss, P. S.; Huang, T. J. Molecular Plasmonics for Biology and Nanomedicine. *Nanomedicine* **2012**, *7*, 751−770.

(14) Galperin, M.; Nitzan, A. Molecular Optoelectronics: The Interaction of Molecular Conduction Junctions with Light. *Phys. Chem. Chem. Phys.* **2012**, *14*, 9421−9438.

(15) Zhang, Q.; Atay, T.; Tischler, J. R.; Bradley, M. S.; Bulovic, V.; Nurmikko, A. V. Highly Efficient Resonant Coupling of Optical Excitations in Hybrid Organic/Inorganic Semiconductor Nanostructures. *Nat. Nanotechnol.* **2007**, *2*, 555−559.

(16) Fofang, N. T.; Park, T.-H.; Neumann, O.; Mirin, N. A.; Nordlander, P.; Halas, N. J. Plexcitonic Nanoparticles: Plasmon-Exciton Coupling in Nanoshell-J-Aggregate Complexes. *Nano Lett.* **2008**, *8*, 3481−3487.

(17) Wiederrecht, G. P.; Wurtz, G. A.; Hranisavljevic, J. Coherent Coupling of Molecular Excitons to Electronic Polarizations of Noble Metal Nanoparticles. *Nano Lett.* **2004**, *4*, 2121−2125.

(18) Wurtz, G. A.; Evans, P. R.; Hendren, W.; Atkinson, R.; Dickson, W.; Pollard, R. J.; Zayats, A. V.; Harrison, W.; Bower, C. Molecular Plasmonics with Tunable Exciton- Plasmon Coupling Strength in J-Aggregate Hybridized Au Nanorod Assemblies. *Nano Lett.* **2007**, *7*, 1297−1303.

(19) Eisele, D. M.; Knoester, J.; Kirstein, S.; Rabe, J. P.; Vanden Bout, D. A. Uniform Exciton Fluorescence from Individual Molecular Nanotubes Immobilized on Solid Substrates. *Nat. Nanotechnol.* **2009**, *4*, 658−663.

(20) Walker, B. J.; Dorn, A.; Bulovic, V.; Bawendi, M. G. Color-Selective Photocurrent Enhancement in Coupled J-Aggregate/Nanowires Formed in Solution. *Nano Lett.* **2011**, *11*, 2655−2659.

(21) Zheng, Y. B.; Kiraly, B.; Cheunkar, S.; Huang, T. J.; Weiss, P. S. Incident-Angle-Modulated Molecular Plasmonic Switches: A Case of Weak Exciton-Plasmon Coupling. *Nano Lett.* **2011**, *11*, 2061−2065.

(22) Zhang, S.; Wei, H.; Bao, K.; Håkanson, U.; Halas, N. J.; Nordlander, P.; Xu, H. Chiral Surface Plasmon Polaritons on Metallic Nanowires. *Phys. Rev. Lett.* **2011**, *107*, 096801.

(23) Coomar, A.; Arntsen, C.; Lopata, K. A.; Pistinner, S.; Neuhauser, D. Near-Field: A Finite-Difference Time-Dependent Method for Simulation of Electrodynamics on Small Scales. *J. Chem. Phys.* **2011**, *135*, 084121.

(24) Henry, A.-I.; Bingham, J. M.; Ringe, E.; Marks, L. D.; Schatz, G. C.; Van Duyne, R. P. Correlated Structure and Optical Property Studies of Plasmonic Nanoparticles. *J. Phys. Chem. C* **2011**, *115*, 9291−9305.

(25) Li, S.; Gao, Y.; Neuhauser, D. Near-Field for Electrodynamics at Sub-Wavelength Scales: Generalizing to an Arbitrary Number of Dielectrics. *J. Chem. Phys.* **2012**, *136*, 234104.

(26) McMahon, J. M.; Li, S.; Ausman, L. K.; Schatz, G. C. Modeling the Effect of Small Gaps in Surface-Enhanced Raman Spectroscopy. *J. Phys. Chem. C* **2012**, *116*, 1627−1637.

(27) Lopata, K.; Neuhauser, D. Multiscale Maxwell-Schrödinger Modeling: A Split Field Finite-Difference Time-Domain Approach to Molecular Nanopolaritonics. *J. Chem. Phys.* **2009**, *130*, 104707.

(28) Lopata, K.; Neuhauser, D. Nonlinear Nanopolaritonics: Finite-Difference Timedomain Maxwell-Schrödinger Simulation of Molecule-Assisted Plasmon Transfer. *J. Chem. Phys.* **2009**, *131*, 014701.

(29) Masiello, D. J.; Schatz, G. C. On the Linear Response and Scattering of an Interacting Molecule-Metal System. *J. Chem. Phys.* **2010**, *132*, 064102.

(30) Arntsen, C.; Lopata, K.; Wall, M. R.; Bartell, L.; Neuhauser, D. Modeling Molecular Effects on Plasmon Transport: Silver Nanoparticles with Tartrazine. *J. Chem. Phys.* **2011**, *134*, 084101.

(31) Sukharev, M.; Nitzan, A. Numerical Studies of the Interaction of an Atomic Sample with the Electromagnetic Field in Two Dimensions. *Phys. Rev. A* **2011**, *84*, 043802.

(32) Mullin, J.; Schatz, G. C. Combined Linear Response Quantum Mechanics and Classical Electrodynamics (QM/ED) Method for the Calculation of Surface-Enhanced Raman Spectra. *J. Phys. Chem. A* **2012**, *116*, 1931−1938.

(33) Sukharev, M.; Galperin, M. Transport and Optical Response of Molecular Junctions Driven by Surface Plasmon Polaritons. *Phys. Rev. B* **2010**, *81*, 165307.

(34) Fainberg, B. D.; Sukharev, M.; Park, T.-H.; Galperin, M. Light-Induced Current in Molecular Junctions: Local Field and Non-Markov Effects. *Phys. Rev. B* **2011**, *83*, 205425.

(35) Zuloaga, J.; Prodan, E.; Nordlander, P. Quantum Description of the Plasmon Resonances of a Nanoparticle Dimer. *Nano Lett.* **2009**, *9*, 887−891.

(36) Morton, S. M.; Silverstein, D. W.; Jensen, L. Theoretical Studies of Plasmonics using Electronic Structure Methods. *Chem. Rev.* **2011**, *111*, 3962−3994.

(37) Song, P.; Nordlander, P.; Gao, S. Quantum Mechanical Study of the Coupling of Plasmon Excitations to Atomic-Scale Electron Transport. *J. Chem. Phys.* **2011**, *134*, 074701.

(38) Mullin, J. M.; Autschbach, J.; Schatz, G. C. Time-Dependent Density Functional Methods for Surface Enhanced Raman Scattering (SERS) Studies. *Comput. Theor. Chem.* **2012**, *987*, 32−41.

(39) Zelinskyy, Y.; May, V. Photoinduced Switching of the Current through a Single Molecule: Effects of Surface Plasmon Excitations of the Leads. *Nano Lett.* **2012**, *12*, 446−452.

(40) Fano, U. Effects of Configuration Interaction on Inensities and Phase Shifts. *Phys. Rev.* **1961**, *124*, 1866−1878.

(41) Luk'yanchuk, B.; Zheludev, N. I.; Maier, S. A.; Halas, N. J.; Nordlander, P.; Giessen, H.; Chong, C. T. The Fano Resonance in Plasmonic Nanostructures and Metamaterials. *Nat. Mater.* **2010**, *9*, 707−715.

(42) Zhang, W.; Govorov, A. O.; Bryant, G. W. Semiconductor-Metal Nanoparticle Molecules: Hybrid Excitons and the Nonlinear Fano Effect. *Phys. Rev. Lett.* **2006**, *97*, 146804.

(43) Artuso, R. D.; Bryant, G. W. Optical Response of Strongly Coupled Quantum Dot- Metal Nanoparticle Systems: Double Peaked Fano Structure and Bistability. *Nano Lett.* **2008**, *8*, 2106−2111 . PMID: 18558787.

(44) Artuso, R. D.; Bryant, G. W. Strongly Coupled Quantum Dot-Metal Nanoparticle Systems: Exciton-Induced Transparency, Discontinuous Response, And Suppression As Driven Quantum Oscillator Effects. *Phys. Rev. B* **2010**, *82*, 195419.

(45) Ridolfo, A.; Di Stefano, O.; Fina, N.; Saija, R.; Savasta, S. Quantum Plasmonics with Quantum Dot-Metal Nanoparticle Molecules: Influence of the Fano Effect on Photon Statistics. *Phys. Rev. Lett.* **2010**, *105*, 263601.

(46) Manjavacas, A.; Abajo, F. J. G. D.; Nordlander, P. Quantum Plexcitonics: Strongly Interacting Plasmons and Excitons. *Nano Lett.* **2011**, *11*, 2318−2323.

(47) Wu, X.; Gray, S. K.; Pelton, M. Quantum Dot-Induced Transparency in a Nanoscale Plasmonic Resonator. *Opt. Express* **2010**, *18*, 23633−23645.

(48) Haug, H.; Koch, S. W. *Quantum Theory of the Optical and Electronic Properties of Semiconductors*; World Scientific: Hackensack, NJ, 2009.

(49) Agranovich, V. M.; Litinskaia, M.; Lidzey, D. G. Cavity Polaritons in Microcavities Containing Disordered Organic Semiconductors. *Phys. Rev. B* **2003**, *67*, 085311.

(50) Salomon, A.; Gordon, R. J.; Prior, Y.; Seideman, T.; Sukharev, M. Strong Coupling between Molecular Excited States and Surface Plasmon Modes of a Slit Array in a Thin Metal Film. *Phys. Rev. Lett.* **2012**, *109*, 073002.

(51) White, A. J.; Galperin, M. Inelastic Transport: A Pseudoparticle Approach. *Phys. Chem. Chem. Phys.* **2012**, 10.1039/C2CP41017F.

(52) Li, G.; Shishodia, M. S.; Fainberg, B. D.; Apter, B.; Oren, M.; Nitzan, A.; Ratner, M. A. Compensation of Coulomb Blocking and Energy Transfer in the Current Voltage Characteristic of Molecular Conduction Junctions. *Nano Lett.* **2012**, *12*, 2228−2232.

(53) Galperin, M.; Nitzan, A. Optical Properties of Current Carrying Molecular Wires. *J. Chem. Phys.* **2006**, *124*, 234709.

(54) Novotny, L.; Hecht, B. *Principles of Nano-Optics*; Cambridge University Press: Cambridge, U.K., 2011.

2743

dx.doi.org/10.1021/jz301139q | *J. Phys. Chem. Lett.* 2012, 3, 2738−2743